

A solitary fibrous tumor arising in the parapharyngeal space, with MRI and FDG-PET findings

メタデータ	言語: eng 出版者: 公開日: 2017-10-05 キーワード (Ja): キーワード (En): 作成者: メールアドレス: 所属:
URL	http://hdl.handle.net/2297/11739

TITLE: Solitary Fibrous Tumour arising in the Parapharyngeal Space

Authors' names and affiliations

Naohiro Wakisaka MD¹, Satoru Kondo MD¹, Akira Tsuji MD¹, Shigeyuki Murono MD¹,

Hiroshi Minato MD², Mitsuru Furukawa MD¹, Tomokazu Yoshizaki MD¹

¹Department of Otolaryngology, School of Medicine, Kanazawa University

²Department of Pathology, School of Medicine, Kanazawa University

Short title: parapharyngeal solitary fibrous tumor

Full address of correspondence author:

Tomokazu Yoshizaki MD

Department of Otolaryngology, School of Medicine, Kanazawa University,

Takara-machi 13-1, Kanazawa, Ishikawa 920-8640, Japan

Phone: +81-76-265-2413

Fax: +81-76-234-4265

e-mail address: tomoy@med.kanazawa-u.ac.jp

TITLE: Solitary Fibrous Tumour arising in the Parapharyngeal Space

ABSTRACT

Solitary fibrous tumour (SFT) is a mesenchymal tumour, which is most often encountered in the pleura. Although the tumour was initially regarded as being derived only from submesothelial fibroblasts and therefore restricted to mesothelial-lined surfaces, recent reports have documented the existence of these lesions at sites unrelated to the serosal surface, including the head and neck. Here, we report a rare case of SFT arising in the parapharyngeal space, which showed interesting features on MRI, CT, and ¹⁸F-fluorodeoxyglucose (FDG) positron emission tomography (PET) findings.

A 38-year-old man presented with a persistent bulging mass at the left oropharyngeal wall. On the CT images, the mass was located in the anterior compartment of the left parapharyngeal space, which showed the heterogenous enhancement on contrast-enhanced CT findings. On MRI, the tumour showed nodule-in-nodule appearance. The inner nodule showed high signal intensities both on T1- and T2-weighted MR images. The entire tumour showed heterogenous enhancement on Gadolinium-enhanced T1-weighted images except for a part of inner nodule. FDG-PET showed the heterogenous radiotracer uptake of FDG in the inner nodule of

the tumour. Gross examination of the surgical specimen showed the nodule-in-nodule like growth pattern. Histologic examinations revealed the admixture of growth patterns including “patternless pattern” and “hemangiopericytoma-like pattern”. The tumour was positive for CD34 and vimentin, but negative for S-100 protein. On the basis of these findings, the final diagnosis was SFT.

Imaging features of SFT arising in the parapharyngeal space are discussed with a review of literatures.

INTRODUCTION

Solitary fibrous tumour (SFT) is a mesenchymal tumour that most frequently occurs in the pleura [1]. Occasionally, SFTs arise at extrapleural sites such as the lung, mediastinum, pericardium and meninges [1-3]. SFTs can also be found in various head and neck sites. Although rare, these locations have included the infratemporal fossa [4], parapharyngeal space [3, 5-12], nose and paranasal sinuses [13, 14], soft palate [15], epiglottis [12], as well as the thyroid [16], parotid [15, 17, 18], and submandibular gland [15, 19].

Here, we report a case of SFT arising in the parapharyngeal space describing the MRI, CT, and ¹⁸F-fluorodeoxyglucose (FDG) positron emission tomography (PET) findings, with a review of literatures.

CASE REPORT

A 38-year-old man presented with a persistent bulging mass at the left side of the oral cavity and a gradually pronounced snoring. He did not have any difficulty swallowing, but symptoms of obstructive sleep apnea. Physical examination revealed a large mucosal covered mass in the left side of the oropharynx. A mobile painless firm mass was also palpable in the left parotid region.

On the CT images, the mass was located in the left parapharyngeal space, which medially displaced the parapharyngeal fat and medial pterygoid muscle, and posterolaterally displaced the carotid sheath, and anteriorly displaced the pterygoid plate. Bony erosion of the mandibular ramus was seen due to the large size of the tumour (Fig. 1A). On the contrast-enhanced CT images, heterogeneous enhancement was observed (Fig. 1B). The parapharyngeal tumour showed nodule-in-nodule appearance on MRI findings. On T1-weighted images, the outer nodule was isointense relative to muscle (Fig. 2A), however, the inner nodule was heterogeneously from iso- to high- signal intensity. On T2-weighted images, the inner nodule was heterogeneously high-signal intensity, which was peripherally surrounded by heterogeneously from iso- to

high-signal intense inner nodule medially (Fig. 2B). The tumour showed heterogeneous enhancement on Gadolinium-enhanced T1-weighted images except for the central part of the inner nodule (Fig. 2C). The corresponding positron emission tomography (PET) shows heterogeneous uptake of FDG in the parapharyngeal tumour. The mass has a mild radiotracer uptake with some round foci of increased activity (Fig. 3). Considering these findings, we diagnosed this case as mesenchymal tumour, especially schwannoma that involved mandibular branch of the trigeminal nerve, and planned the surgical treatment.

A transverse incision was made in the upper neck, and the mass was identified deep in the neck, on the lateral wall of the pharynx. The tumour was firm and the surface was macroscopically smooth and clearly identified. It could be bluntly dissected from surrounding tissue via a transcervical approach.

Gross examination showed the tumour to be a well-defined and round mass with a smooth surface measuring 65 x 50 x 40 mm. The surface of the mass was grayish white and glistening, and it contained small blood vessels. Yellowish white nodule was shown in the fibrous nodule with nodule-in-nodule growth pattern after cutting (Fig. 4A). Histologic examination findings revealed that the tumour was mainly composed of

spindle-shaped cells with varying amounts of collagen (Fig. 4B, D). The tumour cells and collagen tissue arranged in random pattern, known as “patternless pattern” (Fig. 5A). There was moderate pleomorphism, occasional mitoses (1-2/10 high power fields) and prominent vascularity with “hemangiopericytoma-like pattern” (Fig. 5B). Immunohistochemically, the tumour tissue was strongly positive for CD34 and vimentin (Fig. 5C), but negative for S-100. On the basis of these findings, the final diagnosis was a SFT, with benign histologic appearance and areas of cellularity and degeneration (Fig. 4C).

DISCUSSION

SFT, an unusual type of spindle-cell lesion that is most often encountered in the pleura, can be quite difficult to diagnose because of its ability to simulate a variety of soft tissue neoplasms [20]. Although these tumours were initially regarded as being derived only from submesothelial fibroblasts, and therefore restricted to mesothelial-lined surfaces, several recent reports have documented the existence of these lesions at sites unrelated to serosal surfaces, including the liver, lung, mediastinum, upper respiratory tract, thymus, and head and neck [15].

The bland, wavy appearance of the nuclei commonly seen in SFTs may call to mind a neural process such as schwannoma or neurofibroma. The SFTs, however, despite being well circumscribed, are not encapsulated, unlike schwannomas, which will generally display good encapsulation [15]. The lesions are characterized by a variegation of growth patterns. The tumours commonly show narrow cords of cells with interspersed thick bundles of collagen (patternless pattern), admixed with areas that showed a prominent hemangiopericytoma-like and angiofibroma-like appearance, neural-type fascicular areas with wavy nuclei, and occasional herring-bone formation.

Cellularity of tumour varies from area to area and is inversely related to the amount of collagen [15, 20]. Immunohistochemically, SFTs appear to demonstrate a mesenchymal, nonepithelial phenotype by showing strong vimentin reactivity and by being almost invariably negative for cytokeratin and S-100 protein [21]. CD34, a myeloid progenitor cell antigen that is also present in normal and neoplastic endothelial cells and in some other mesenchymal cells, including subsets of fibroblasts, is strongly positive in most cases of SFT, showing not only endothelial cell reactivity but also positivity in the neoplastic spindle cells [21-23]. In the present case, immunohistochemical study showed positive staining of spindle cells for CD34 and vimentin, but negative for cytokeratin and S-100 protein. Thus, the present case was diagnosed as SFT from both histological and immunohistochemical findings.

It is reported that mature fibrous tissue usually has lower signal intensity on the T1- and T2- weighted images, and this is related to the area of hypocellularity, and the abundant collagen stroma [24, 25]. In the present case, the tumour showed nodule-in-nodule appearance on MRI. The hypocellular, but more collagenous outer nodule in the tumour corresponded to the lower signal intensities both on T1- and

T2-weighted images compared with hypercellular, but less collagenous inner nodule. It has also been reported that intense enhancement of pleural SFTs is due to its high vascularity [26, 27]. Lee et al. reported that the intratumoral low attenuation areas on T1-weighted images correlated with myxoid or cystic degeneration [28]. All these previous reports explain the compatibility of the MRI findings with the histological findings of high vascularity and partial degeneration in the present case. Finally, our FDG-PET findings showed hot areas in the inner nodule of the tumour, a hypercellular and less collagenous area.

The imaging features of previously reported nine SFTs of parapharyngeal space are summarized in the Table. On MRI, all SFTs showed heterogeneously high intensity on the T2-weighted images. On contrast-enhanced T1-weighted images, heterogenous enhancement was observed in four of five parapharyngeal SFTs and homogenous enhancement in one. On the contrast-enhanced CT images, heterogenous enhancement was observed in all SFTs arising in the parapharyngeal space. Thus, these findings are characteristic of SFTs in the parapharyngeal space, however, CT & MRI findings specific for parapharyngeal SFTs were not found.

CONCLUSION

A case of SFT arising in the parapharyngeal space was reported.

The tumour showed nodule-in-nodule appearance on MRI. The outer nodule, corresponding to the hypocellular but more collagenous area, showed the lower signal intensities on T1- and T2-weighted MRI compared with inner nodule, corresponding to the hypercellular but less collagenous area. The tumour showed strong enhancement on Gadolinium-enhanced MRI, with intratumoral low attenuation area corresponding to the degeneration.

The imaging features of SFTs arising in the parapharyngeal space were summarized. Common MRI and CT findings of parapharyngeal SFTs were found, however, these findings were not specific for SFTs in the parapharyngeal space.

REFERENCES

1. England DM, Hochholtzer L, McCarthy MJ. Localized benign and malignant fibrous tumors of the pleura: a clinicopathological review of 223 cases. *Am J Surg Pathol* 1989;23:640-58.
2. Goodlad JR, Fletcher CD. Solitary fibrous tumor arising at unusual sites: analysis of a series. *Histopathology* 1991;19:515-22.
3. Kim HJ, Lee HK, Seo JJ, Kim HJ, Shin JH, Jeong AK, Lee JH, *et al.* MR imaging of solitary fibrous tumors in the head and neck. *Korean J Radiol* 2005;5:136-42.
4. Rayappa CS, McArthur PD, Gangopadhyay K, Antonius JI. Solitary fibrous tumour of the infratemporal fossa. *J Laryngol Otol* 1996;110:594-7.
5. Hashimoto D, Inoue H, Ohbayashi C, Nibu K. Solitary fibrous tumor in the parapharyngeal space. *Otolaryngol Head Neck Surg* 2006;134:535-6.
6. Cizmarevic B, Lanisnik B, Didanovic V, Kavalari R. Solitary fibrous tumor of the parapharyngeal space.
7. Jeong AK, Lee HK, Kim SY, Cho KJ. Solitary fibrous tumor of the parapharyngeal space: MR imaging findings. *Am J Neuroradiol* 2002;23:473-5.

8. Galera-Ruiz H, Martinez-Pozo A, Alos LL, Cardesa A, Traserra J. Single fibrous tumor of the parapharyngeal space. *Acta Otorrinolaringol* 2000;51:457-9.
9. Sato J, Asakura K, Yokoyama Y, Satoh M. Solitary fibrous tumor of the parotid gland extending to the parapharyngeal space. *Eur Arch Otorhinolaryngol* 1998;255:18-21.
10. Gangopadhyay K, Taibah K, Manohar MB, Kfoury H. Solitary fibrous tumor of the parapharyngeal space: A case report and review of the literature. *Ear Nose Throat J* 1996;75:681-4.
11. Al-Sinawi A, Johns AN. Parapharyngeal solitary fibrous tumour: an incidental finding at ENT examination. *J Laryngol Otol* 1994;108:344-7.
12. Safneck JR, Alguacil-Garcia A, Dort JC, Phillips SM. Solitary fibrous tumour: Report of two new locations in the upper respiratory tract. *J Laryngol Otol* 1993;107:252-6.
13. el-Naggar AK, Weard RM, Ro JY, Ayala AG, Ordonez NG. Fibrous tumor with hemangiopericytic pattern, so-called "localized fibrous tumor of the pleura". *Lab Invest* 1987;56:21.

14. Zukerberg LR, Rosenberg AE, Randolph G, Pilch BZ, Goodman ML. Solitary fibrous tumor of the nasal cavity and paranasal sinuses. *Am J Surg Pathol* 1991;15:126-30.
15. Suster S, Nascimento AG, Miettinen M, Sickel JZ, Moran CA. Solitary fibrous tumors of soft tissue. A clinicopathologic and immunohistochemical study of 12 cases. *Am J Surg Pathol* 1995;19:1257-66.
16. Taccagni G, Sambade C, Nesland J, Terreni MR, Sobrinho Simos M. Solitary fibrous tumour of the thyroid: clinicopathological, immunohistochemical and ultrastructural study of three cases. *Virchows Arch* 1993;422:491-7.
17. Ferreiro JA, Nascimento AG. Solitary fibrous tumour of the major salivary glands. *Histopathology* 1996;28:261-4.
18. Hanau CA, Miettinen M. Solitary fibrous tumor: histological and immunohistochemical spectrum of benign and malignant variants presenting at different sites. *Hum Pathol* 1995;26:440-9.
19. Gunhan O, Yildiz FR, Celasun B, Onder T, Finci R. Solitary fibrous tumour arising from sublingual gland: report of a case. *J Laryngol Otol* 1994;108:998-1000.

20. Moran CA, Suster S, Koss MN. The spectrum of histologic growth patterns in benign and malignant fibrous tumors of the pleura. *Sem Diagn Pathol* 1992;9:169-80.
21. Hanau CA, Miettinen M. Solitary fibrous tumor: Histological and immunohistochemical spectrum of benign and malignant variants presenting at different sites. *Hum Pathol* 1995;26:440-9.
22. Traweek ST, Kandalaf PL, Mehta P, Battifora H. The human hematopoietic progenitor cell antigen (CD34) in vascular neoplasia. *Am J Clin Pathol* 1991;96:25-31.
23. Nicholoff BJ. The human progenitor cell antigen (CD34) is localized on endothelial cells, dermal dendritic cells, and perifollicular cells in formalin-fixed normal skin, and on proliferating endothelial cells and stromal spindle cells in Kaposi's sarcoma. *Arch Dermatol* 1991;127:523-9.
24. Ferretti GR, Chiles C, Cox JE, Choplin RH, Coulomb M. Localized benign fibrous tumors of the pleura: MR appearance. *J Comput Assist Tomogr* 1997;21:115-120.
25. Kransdorf MJ, Jelinek JS, Moser RP Jr, Utz JA, Hudson TM, Neal J, et al. Magnetic

- resonance appearance of fibromatosis. A report of 14 cases and review of the literature. *Skeletal Radiol* 1990;19:495-499.
26. Tateishi U, Nishihara H, Morikawa T, Miyasaka K. Solitary fibrous tumor of the pleura: MR appearance and enhancement pattern. *J Comp Assist Tomography* 2002;26:174-9.
27. Martin AJ, Fisher C, Igbaseimokumo U, Jarosz JM, Dean AF. Solitary fibrous tumor of the meninges: case series and literature review. *J Neurooncol* 2001;54:57-69.
28. Lee KS, Im J-G, Choe KO, Kim CJ, Lee BH. CT findings in benign fibrous mesothelioma of the pleura: pathologic correlation in nine patients. *Am J Roentgenol* 1992;158:983-986.

FIGURE LEGENDS

Fig. 1. Plain and contrast-enhanced CT findings. (A) Plain CT. The tumour is located in the anterior compartment of the left parapharyngeal space. The mass displaced the parapharyngeal fat medially. Ramus mandibulae was thinned due to the large size of the tumour. (B) Contrast-enhanced CT. Heterogenous enhancement of the tumour was observed. The mass displaces the carotid sheath posterolaterally.

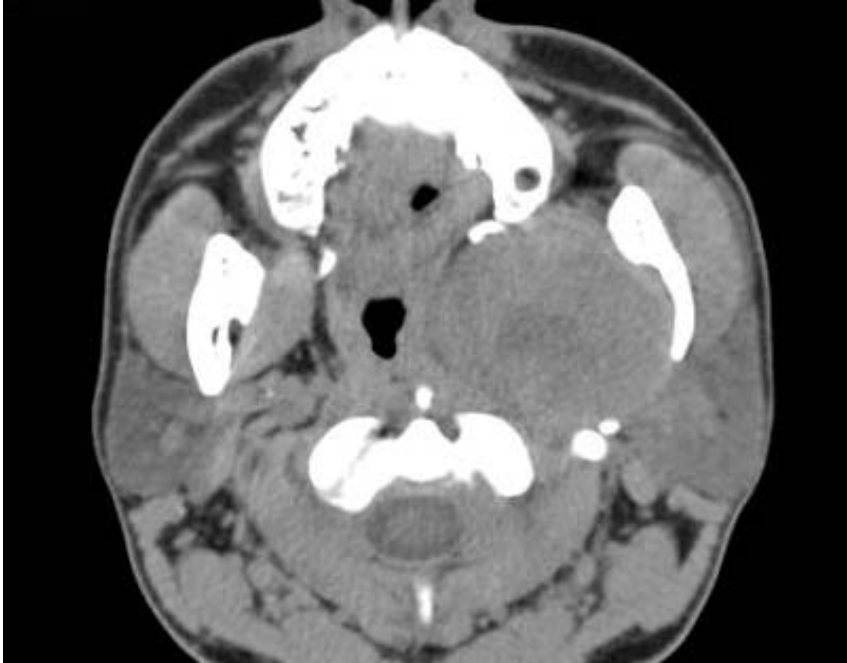
Fig. 2. MRI findings. Parapharyngeal tumour showed nodule-in-nodule appearance. (A) Axial and coronal T1-weighted MRI. Inner nodule appeared heterogeneously from iso- to high- signal intensity. (B) Axial and coronal T2-weighted MRI. Inner nodule showed heterogeneously high signal intensity. Outer nodule appeared from iso- to high-signal intensity. (C) Axial and coronal Gadlinium-enhanced T1-weighted MRI showed the strong enhancement of the tumour except for a part of the inner nodule.

Fig. 3. ¹⁸F-fluorodeoxyglucose (FDG) positron emission tomography (PET) findings show the heterogeneously increased uptake of FDG in the tumour at the left

parapharyngeal space. (A) Axial Image. (B) Coronal image.

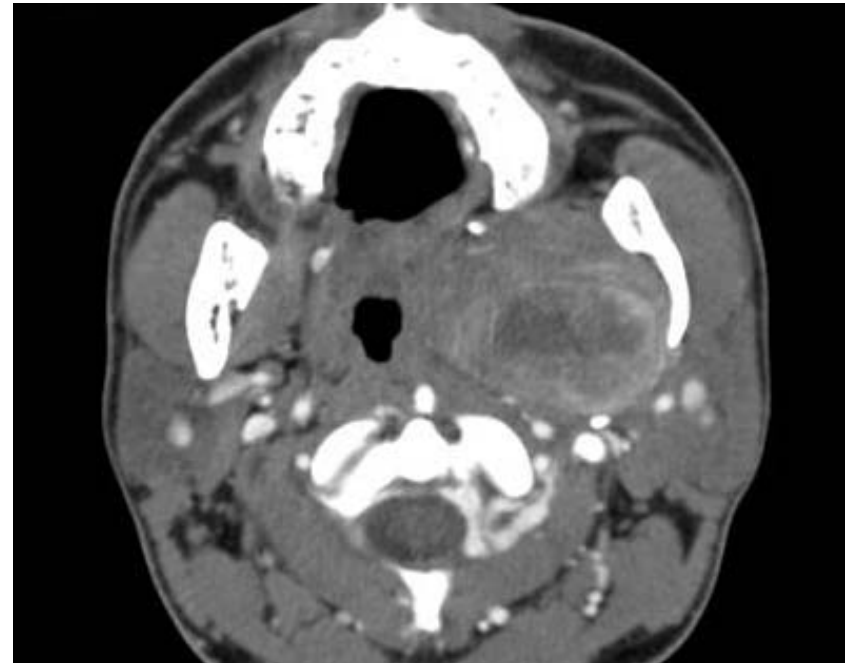
Fig. 4. (A) Gross examination of the tumour showed the nodule-in-nodule growth pattern. (B) Microscopic examination of the inner nodule showed hypercellular, but less collagenous histology. A part of the inner nodule showed the area with degeneration (C). (D) The outer nodule showed hypocellular, but more collagenous area, in contrast to the inner nodule.

Fig. 5. The admixture of two or more growth patterns within the same lesion is characteristic histological feature of solitary fibrous tumour. (A) The tumour is composed of narrow cords of cells with interspersed thick bundles of collagen (patternless pattern). (B) Tumour cells are arranged around collapsed, irregular, branching capillaries and large vessels. (C) Immunohistochemical staining of the tumour with anti-CD34, a myeloid progenitor cell antigen, showed strong immunoreactivity in the tumour cells.



Plain CT

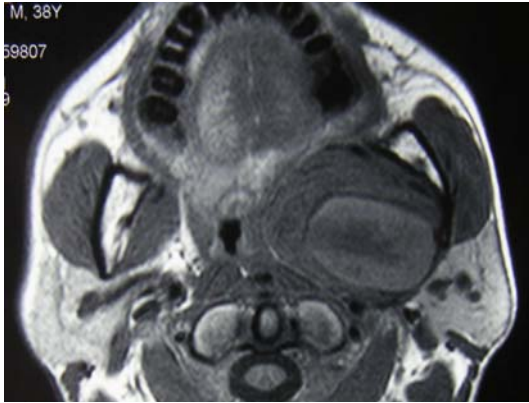
A



Enhanced CT

B

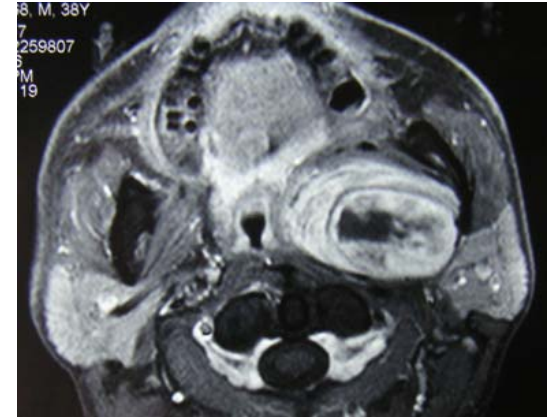
Fig. 1



T1 Axial



T2 Axial

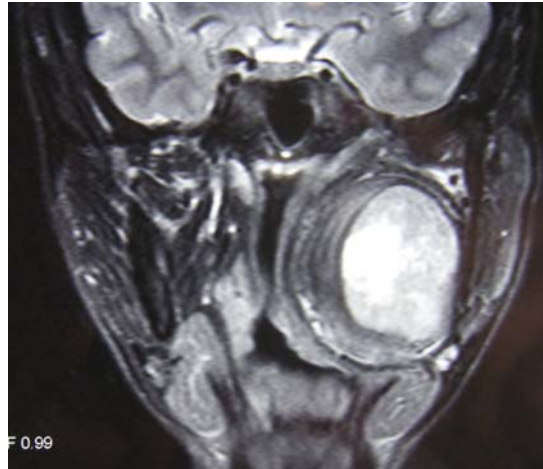


Gd-T1 Axial



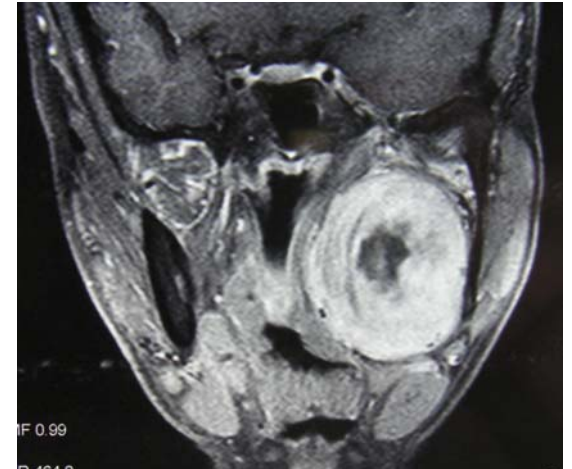
T1 Coronal

A



T2 Coronal

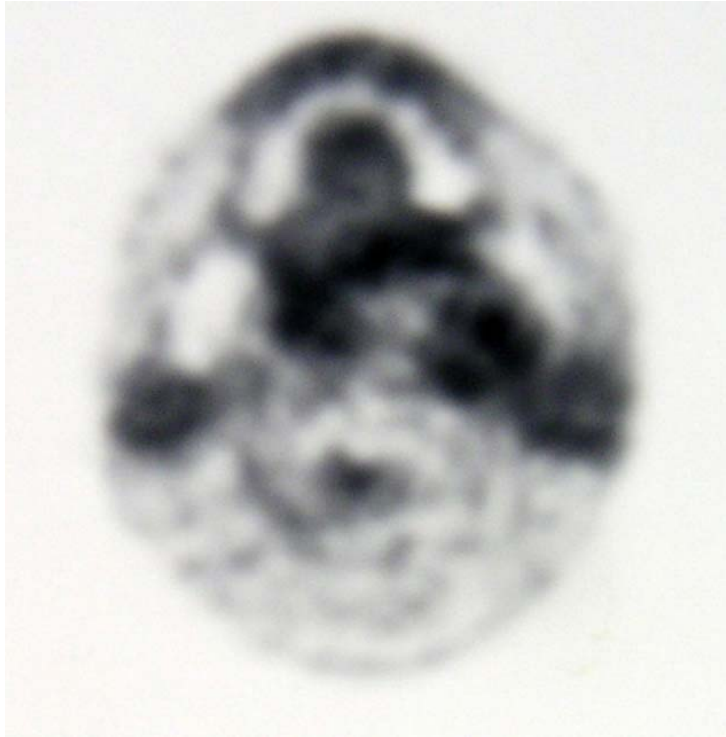
B



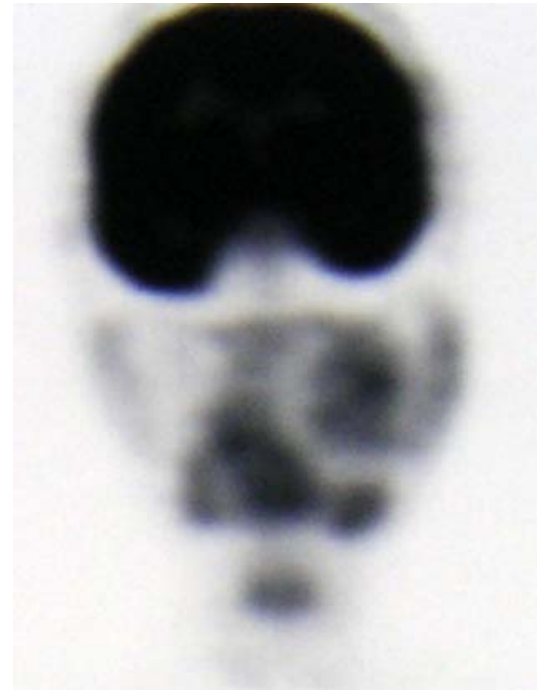
Gd-T1 Coronal

C

Fig. 2



Axial



Coronal

Fig. 3

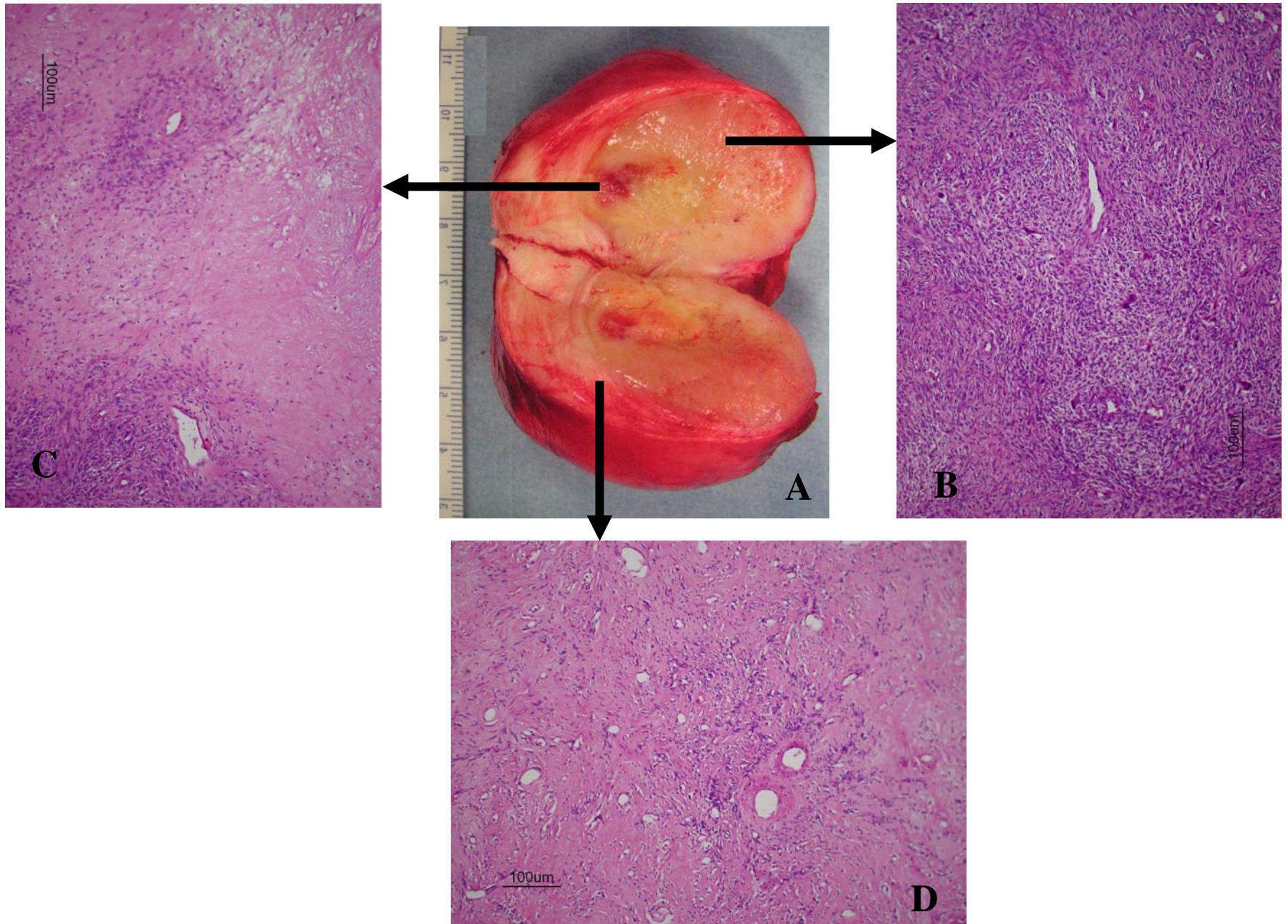
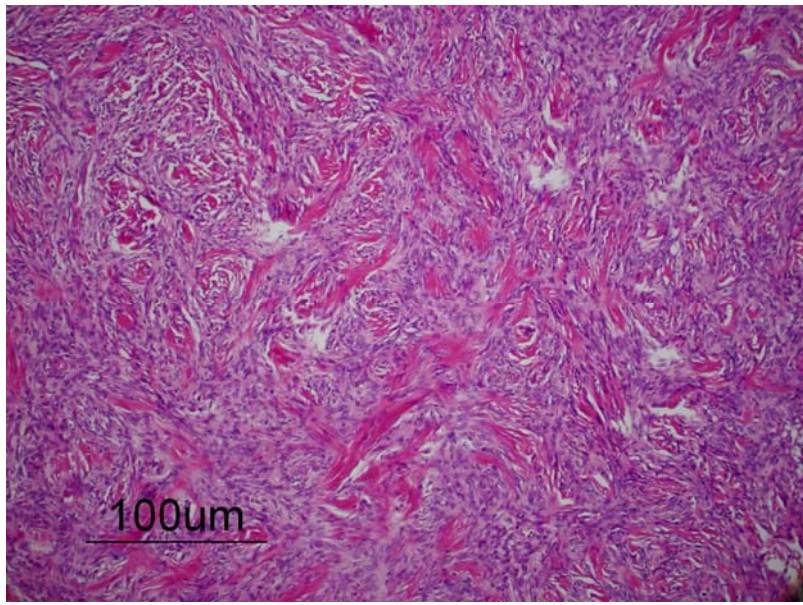
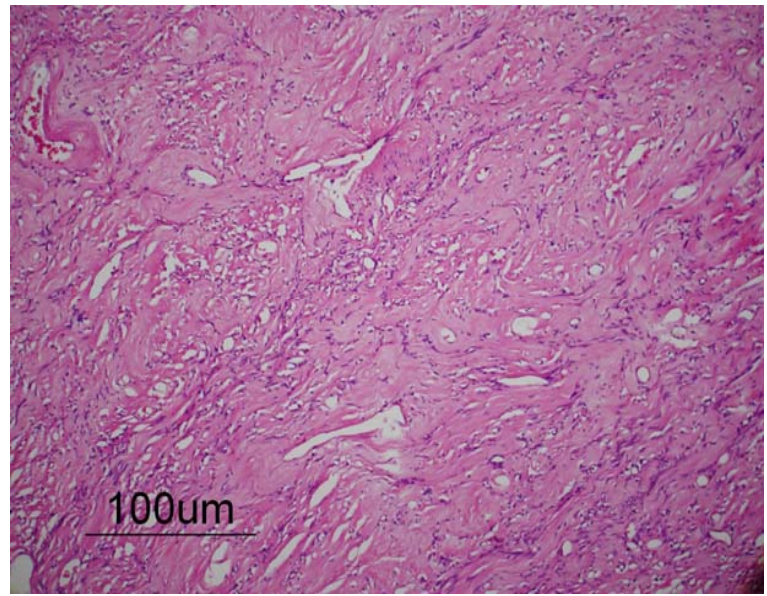


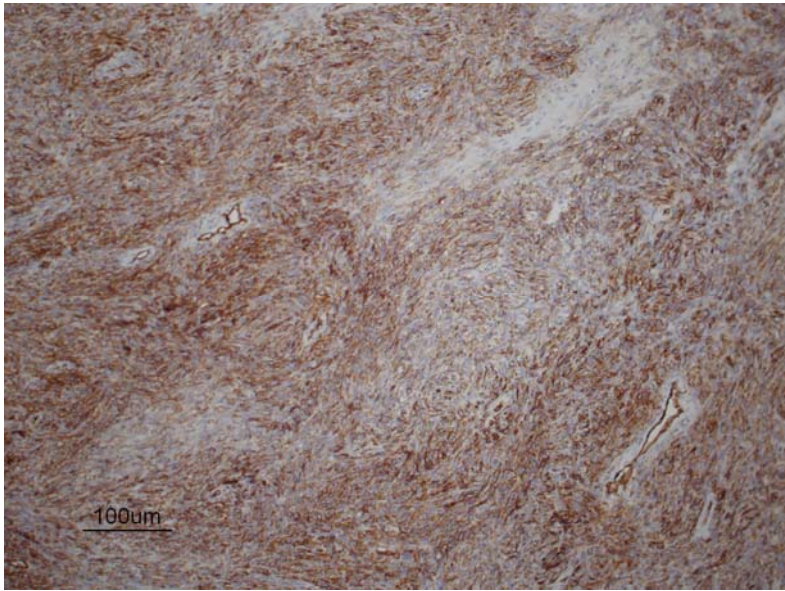
Fig. 4



A



B



C

Fig. 5

Table: CT & MRI findings of solitary fibrous tumours arising in the parapharyngeal space

Author (Reference No.)	CT Findings	MRI Findings
Safneck, <i>et al.</i> (12)	heterogenous enhancement	ND
Al-Sinawi, <i>et al.</i> (11)	ND	Gd-T1 : heterogenous enhancement
Gangopadhyay, <i>et al.</i> (1)	heterogenous enhancement	ND
Sato, <i>et al.</i> (9)	heterogenous enhancement	T1: hypointensity T2: heterogeneously high intensity Gd-T1 : heterogenous enhancement
Jeong, <i>et al.</i> (7)	ND	T1: isointensity T2: heterogeneously high intensity Gd-T1: homogenous enhancement
Cizmarevic, <i>et al.</i> (6)	heterogenous enhancement	T2: heterogeneously high intensity
Kim, <i>et al.</i> (3)	ND	T1: isointensity T2: heterogeneously high intensity Gd-T1: homogenous enhancement
Hashimoto, <i>et al.</i> (5)	heterogenous enhancement	T1: homogeneously high intensity T2: heterogeneously high intensity
Wakisaka, <i>et al.</i>	heterogenous enhancement	T1: hypo-isointensity T2: heterogeneously high intensity Gd-T1 : heterogenous enhancement

ND: not done; Gd: Gadolinium-enhanced.